



## Biosorption of Lead (II) and Aluminum (III) From Real Water Samples Onto Precursor Pistachio Shells: Adsorption Characteristics, Kinetics and Thermodynamic Studies

Mohammed M.H Al-Awadhi<sup>1</sup>, Mohammed S. A. Bashanaini<sup>2</sup> and Magda A Akl<sup>\*2</sup>

<sup>1</sup>Department of Chemistry, Faculty of Education & Science, Saba Region University, Marib, Yemen

<sup>2</sup>Department of Chemistry, Faculty of Science, Mansoura University, Mansoura, Egypt



### Abstract

In this study, low-cost biosorbent has been produced from the precursor pistachio shells (PPS). The physicochemical properties, and chemical composition of PPS and the active surface functional groups involved in adsorption were identified using BET and N<sub>2</sub> adsorption isotherm, pH<sub>PZC</sub> and FTIR. The PPS biosorbent was applied for the elimination of lead (II) and aluminum (III) from real water samples, where the efficiency was evaluated as functions of pH value, the initial Pb(II) and Al (III) amount, concentration of adsorbent, adsorption time, temperature and co-existing ions. The results showed that the PPS biosorbent showed excellent adsorption efficiencies towards Pb(II) and Al(III) with a maximum adsorption capacity of 35.08 and 12.77 mgg<sup>-1</sup>, for Pb(II) and Al(III), respectively. The adsorption kinetic and isotherm reflect that the adsorption of Pb(II) and AL(III) onto PPS biosorbent obeyed pseudo-2-order and Langmuir isotherm model, respectively. An endothermic and spontaneous adsorption process of Pb(II) and AL(III) was confirmed by the calculated thermodynamic functions.

**Keywords:** Precursor Pistachio shells, Kinetic studies, Adsorption, Lead (II) and Aluminum (III)

### 1. Introduction

The major source of lead within the environment is from plastics, wrapping up apparatuses, cathode beam tubes, ceramics, fastens pieces of lead blazing and other minor item, steel and cable reclamation. Lead can result within the wide extend of biological impacts depending upon the level and length of presentation [1]. Within the environment, lead ties emphatically to particles such as oil, silt and sewage slime so its evacuation is of awesome concern [2]. Aluminum is the foremost copious metal within the earth's crust [3,4]. In acidic situations aluminum is discharged as Al (III) ions [5], which are inalienably harmful to numerous organisms [6]. After coagulation, flocculation and filtration there will be a few leftover broken down aluminum within the treated water [7]. It is presently well known that this metal is toxic to a variety of living beings [ 8-11]. The heavy metals, having unsafe impacts on wellbeing and environment, can be treated from

wastewater by utilizing different physicochemical strategies [12]. Adsorption, precipitation, phytoextraction, ultrafiltration, reverse osmosis, and electro dialysis are the foremost habitually favored strategies [13]. Among them, adsorption gets significant intrigued with the tall effectiveness in heavy metal expulsion. Adsorption has illustrated its proficiency and financial achievability as a wastewater treatment handle compared to the other filtration and partition strategies, and has picked up significance in mechanical applications [14]. Activated carbon is the foremost commonly utilized adsorbent within the adsorption forms due to its increased adsorption capacity, high surface range, and increased degree of surface reactivity, while, it encompasses a generally increased cost, increased operation costs, and issues with recovery for the mechanical scale applications [15]. This driven to a look coordinated to creating low-cost and locally accessible adsorbent materials with greatest

\*Corresponding author e-mail: [magdaakl@yahoo.com](mailto:magdaakl@yahoo.com); (Prof. Magda Akl).

EJCHEM use only; Received date 29 December 2022; revised date 06 January 2023; accepted date 18 January 2023

DOI: 10.21608/EJCHEM.2023.184259.7401

©2023 National Information and Documentation Center (NIDOC)

adsorption capacity [16, 17]. A wide assortment of materials such as bark/tanin-rich materials, lignin, chitin, chitosan, dead biomass, sawdust, peat greenery, adjusted fleece, altered cotton [18], banana essence [19], rice husk [20], and leaves [21] are being utilized as substituted options to costly adsorbents.

The objectives of the present study can be represented as:

- i) Design, preparation and characterization of pistachio shell derived biosorbent (PPS) using BET and N<sub>2</sub> adsorption isotherm, pH<sub>PZC</sub> and FTIR.
- ii) Batch sorption experiments utilizing Pb (II) and Al (III) as pollutants.
- iii) Investigating the ideal factors like pH, the initial metal ion amount, adsorbent mass, temperature, isotherms, thermodynamics, and oscillation time.
- iv) Elucidation of adsorption kinetics, thermodynamic, isotherm and desorption studies.

## 2.1. Experimental

### 2.2. Materials and solutions

The stock solution 1000 mg/L of lead ion as adsorbate was prepared by dissolving 1.5984 g of Pb(NO<sub>3</sub>)<sub>2</sub> (supplied by Sigma-Aldrich (Germany)) in 1000 mL of solution using acidified doubled distilled water.

The stock solution 1000 mg/L of aluminum adsorbate was prepared by dissolving 8.9426 g of AlCl<sub>3</sub>.6H<sub>2</sub>O [supplied by Sigma-Aldrich (Germany)] in 1000 mL of solution using acidified doubled distilled water.

### 2.3. Instrumentation

The surface area of the adsorbent was obtained from N<sub>2</sub> adsorption measurements made at 77K and using the BET equation. Chemical functional groups present in PPS were examined before and after metal ion adsorption using Nicolet FTIR spectrophotometer. The type and amount of functional groups on the PPS were determined using Surface acidity and Boehm titration techniques.

The moisture content is determined by heating 0.05 g of the adsorbent in an oven at (110) °C overnight and then it was cooled to room temperature in desiccators and then weighed. The ash content of the prepared adsorbent is determined to measure minerals present as impurities in the adsorbent which remain upon burn off of the carbonaceous portion during pyrolysis. About 0.5 g of adsorbent was put in muffle furnace for about 6 h at 700 °C and then the final weight was recorded. The pH<sub>PZC</sub> was determined as it is reported in previous work. The pH of solutions was determined using aHANNA pHmeter (Hi 931401,

Portugal). The batch sorption experiments were carried out at 240 rpm on a Shaking Water Bath (Nickel Electro Ltd., NE5, UK). The amounts of lead and aluminum were analyzed using UV-Vis spectrophotometer (Chrom Tech., Ltd., and USA) at 520 nm using PAR and at 535 nm for Al<sup>3+</sup> using ECR as a complexing agent, respectively.

### 2.4. Preparation of precursor of pistachio shells

The precursor of pistachio shells (PPS) was first washed free of dirt and inherent pulp portion, and dried in an electric oven at 110 °C for 24 h. The dried shells were crushed to give a pale yellow semi powder which became easy to weight and impregnate and then sieved and particles of 0.063-0.500 mm size were used as adsorbent (PPS).

### 2.5. Batch test

Batch tests were performed by stirring 0.025 g of PPS with 25 mL H<sub>2</sub>O solution of metal ion solution in 250 mL Erlenmeyer flasks placed in thermostated water bath shaker at different concentrations (1 -45 mg/L) of Al<sup>3+</sup> and (5- 100) mg/L of Pb<sup>2+</sup>, pHs (2-7), temperatures (27.0 °C - 47.0 °C), doses of PPS (0.005 - 0.0625 g) and NaCl concentrations (5- 200 mmole/L) at the range of shaking rate of 200-220 rpm.

The maximum adsorption capacity of metal ion removed by PPS (qm), and the metal ions removal percentage (R %) are determined using Eqs. (1) &(2):

$$q_m = \frac{(C_o - C_e)}{m} \times V \quad (1)$$

$$R \% = \frac{(C_o - C_e)}{C_o} \times 100 \quad (2)$$

Where qm is the maximum adsorption capacity (mgg<sup>-1</sup>), C<sub>o</sub> and C<sub>e</sub> are the initial and equilibrium state concentrations of the metal ions (mg/L), m is the mass of the adsorbent used (g) and V is the solution volume of the metal ions (mL), respectively.

### 2.5. Desorption Studies

Desorption tests were performed using various desorbing agents: absolute ethanol, HNO<sub>3</sub>, HCl, NaOH and NaHCO<sub>3</sub> with concentrations between (0.01 to 0.5 M). Briefly, 0.2 g of PPS loaded Pb (II) or PPS loaded Al (III) was immersed in 10mL of eluent solution for 72 h with shaking at 150 rpm. The bulk solute concentration in solution was measured as previously described. Then the desorbed metal ion concentration was analyzed spectrophotometrically after the suspension was shaken for a fixed time. The desorption efficiency (D, %) of Pb and Al can be calculated using equation, Eq. 3

$$\frac{\text{Desorption}}{\text{Total Adsorbed amount of PB(II) AND AL(III)}} \times 100\% (3)$$

Where  $q_d$  and  $q_a$  are the desorption capacity ( $\text{mgg}^{-1}$ ) and adsorption capacity, respectively.

### 3. Results and discussion

#### 3.1. Characterization of PPS

##### 3.1.1. Surface pH, $\text{pH}_{\text{PZC}}$ and moisture %:

The adsorbent may contain various elements originating from the raw material or generated during

**Table 1**

Physicochemical parameters of PPS

Acidic groups (mmol/g)				Basic groups (mmol/g)	Surface pH	$\text{pH}_{\text{PZC}}$	Moisture content %	Ash content %
Carboxylic	Lactonic	Phenolic	Total					
0.626	3.632	0.747	5.005	0.740	6.37	6.57	3.810	0.691

The surface pH of PPS introduces a valuable indication for nature of the functional groups found on the PPS surface. In solution, bronsted acidic groups of the carbon surface tend to give their protons to  $\text{H}_2\text{O}$  molecules and hence the charge of the surface becomes negative. Alternatively, Lewis bases accepted protons from solution becoming positively charged. It is known that most of the oxygen containing functionalities behaves as bronsted acids, donating protons to the aqueous media and so being responsible for  $\text{pH} < 7$  of carbons [22]. However, the basic characters come from two types of contributions; the adsorption of protons by the aromatic basal planes of the carbons and by surface complexes (i.e., pyrone-like structures) [20]. The pH of the slurries of PPS was found to be 6.37. This may be taken as evidence that acid functional groups slightly predominate on the surface of PPS. The  $\text{pH}_{\text{PZC}}$  is the pH at which the net surface charge equals to zero. [23]. It allows quantifying the acidic or basic character of the carbon. The  $\text{pH}_{\text{PZC}}$  and the pH of the solution determine the charge on the surface that will be present; the carbon surface is +vely charged and surface sites are protonated at

modification and manufacture, the quantity of these elements (e.g., useless minerals) may be varied from 1 to 20 %. These elements are often the content so called ash content decreased to 0.1 to 0.2 %. The elements other carbon is the responsible for determining surface properties like surface pH, point of zero charge and the functional groups of the PPS. Table 1 summarized the surface characterization of the PPS and the moisture and ash content of precursors pistachio shells (PPS).

$\text{pH} < \text{pH}_{\text{PZC}}$  and, but at  $\text{pH} > \text{pH}_{\text{PZC}}$  is -vely charged. [24]. The  $\text{pH}_{\text{PZC}}$  value of PPS is 6.57 as shown in Table 1.

##### 3.1.2. FTIR spectra

The IR spectrum of the precursor (natural pistachio shells; PPS) is presented in (Fig. 1a, b). The data indicate existence of bands at 3422, 1741, 1600(sh), 1540(sh), 1512 and 1056  $\text{cm}^{-1}$  attributed to the presence of OH (phenolic and/or carboxylic), COOH, C=C, C=N and C-N groups, respectively. The IR spectrum of the precursor pistachio shell PPS with Pb(II) is shown in (Fig. 1a). The data shows that the bands at 2066, 1383 and 1337  $\text{cm}^{-1}$  assigned to the lactonic OH groups are shifted to lower wavenumbers in comparing to the spectrum of PPS alone (Fig. 1a,b) which are observed at 2128, 1377 and 1333  $\text{cm}^{-1}$ , respectively. Fig. 1b illustrates the IR spectrum of the PPS loaded with  $\text{Al}^{3+}$  ion. The results show the observation of new bands at 1655 and 1598  $\text{cm}^{-1}$  assigned to  $\nu$  (COOH) vibration. Also, the bands at 1598 and 1510  $\text{cm}^{-1}$  are assigned to  $\nu$  (COOH) vibration. These [25].bands are obscured in the IR spectrum of PPS (Fig. 1b) due to the destruction of hydrogen bond. Bands at 438 and 407  $\text{cm}^{-1}$  are assigned to  $\nu$ (Al-O) and  $\nu$ (Al-N) vibration, respectively[26].

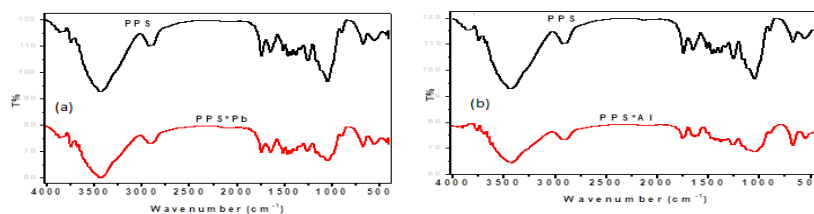


**Fig. 1:** FTIR spectra of (a) [PPS and PPS\*Pb] (b) [PPS and PPS\*Al]

### 3.2. Adsorption of Pb (II) and Al (III) onto PPS

#### 3.2.1. Influence of pH

Fig. 2 shows the effect of pH on Pb(II) and Al(III) ion adsorption onto PPS. It is noted that Pb(II) and Al(III) ion uptake gradually increases with the increase of pH of Pb(II) and Al(III) ion solution from pH 2 to (3 and 5) and it reaches its maximum pH at (4-7 and 6-7) for PPS. In acidic medium (pH < 2) the lower removal metal ion is likely due to the presence of metal in solution as free  $Mn^+$  ions competing with prorogated sorption sites of adsorbents (-COO and -NH<sub>2</sub>). Moreover, this leads to the electric of reptation between  $Mn^+$  ions and the functional groups which possess positively charged on the surface of PPS. The PPS surface with increasing pH of the solution, begin to be greet negatively charged because of increases of OH- groups, this leads to further electrostatic interaction of ions of  $Mn^+$  with negative functional groups and facilitates the adsorption of  $Mn^+$  ions. The determination of  $Pb^{2+}$  and  $Al^{3+}$  was possible to carry out at pH 5-7 and 4-7, respectively. Therefore, this pH range was selected as the working pH for subsequent work.

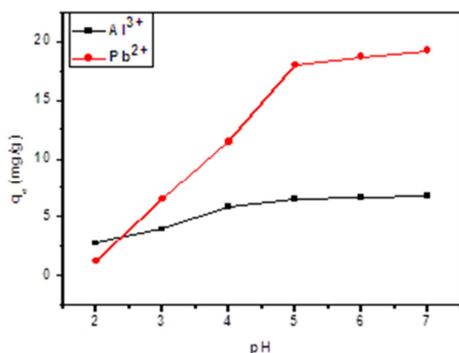


Fig. 2: Influence of pH on removal of Pb (II) ( $C_i = 25 \text{ mgL}^{-1}$ ) & Al (III) ( $C_i = 8 \text{ mgL}^{-1}$ ) ionon PPS

#### 3.2.2. The impact of initial metal amount

The influence of start metal ion amount on the sorption capacity of PPS towards Pb (II) and Al (III) is displayed in Figure 3. It is demonstrated that the amount of Pb (II) or Al (III) adsorbed per unit mass of PPS increases with increasing initial metal ion concentration in the sample solution. The start amount of metal ions increases from 5 to 100  $\text{mgL}^{-1}$  and from 1 to 45  $\text{mgL}^{-1}$  for Pb(II) and Al(III) at 27°C. At equilibrium ( $q_e$ ), the amount adsorbed increases from 4.89 to 35.90  $\text{mgg}^{-1}$  and from (0.977 to 12.473  $\text{mgg}^{-1}$  for Pb(II) and Al(III), respectively.

This may be accounted for by the fact that the rise in the start amount of adsorbate works as a driving

force to overcome the metal ion's mass transfer resistance between the solid and aqueous phases. [27] At higher Pb (II) and Al (III) ions amounts, adsorption capacity reaches a plateau indicating saturation of available functional groups on PPS

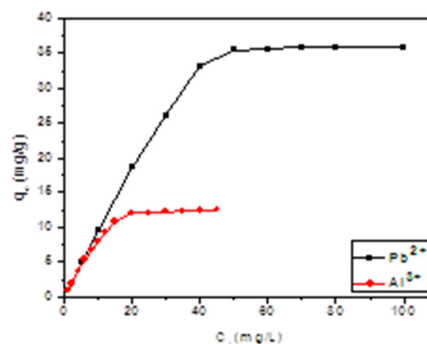


Fig. 3: Influence of initial amount of Pb(II) and Al(III) ions on the adsorption capacity of PPS

#### 3.2.3. Influence of PPS mass

Figure 4 shows the influence of PPS mass on the removal of Pb(II) and Al(III) from aqueous solutions. The removal of metal ion is changed with the change of PPS dose and it rises with a rise in mass of PPS. The removal % of Pb(II) and Al(III) ions by PPS increased rapidly with increase in dose of adsorbent up to 0.025 g, then gradually increased with further increment in dose of adsorbent up 0.05 g and thereafter remained unchanged. The R % of Pb(II) and Al(III) ions increased from (54.34 % to 81.72 %) and (37.38 % to 96.28 %) as the mass of PPS raised from (0.005 to 0.0625 g), respectively. The rise in the amount of metal ion adsorbed may be because of the increase in the available adsorption surface groups. [28].

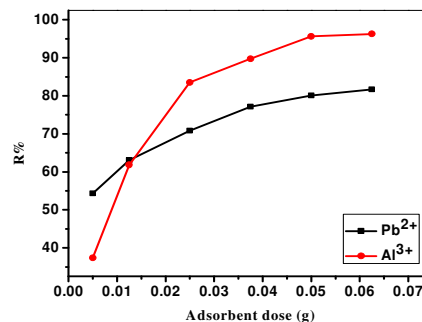


Fig. 4: Influence of PPS mass on removal% of Pb(II) ( $C_i = 50 \text{ mgL}^{-1}$ ) and Al(III) ( $C_i = 8 \text{ mgL}^{-1}$ ) on PPS.

#### 3.2.4. Influence of contact time

The influence of contact time on the adsorption of Pb(II) and Al(III) onto PPS is presented in Figure 5. The shapes of kinetics curves are similar and formed of a rapid start removal followed by a slow diffusion reaching a plateau. This can be explained by the larger surface area present at the start for the removal of Pb(II) and Al(III) onto PPS. Thus, about 80% of adsorption capacity of Pb(II) and Al(III) is attained within the first 60min. The adsorption of the Pb(II) and Al(III) on the PPS reaches equilibrium after 120 min. A contact time of 120 min was used in the following experiments.

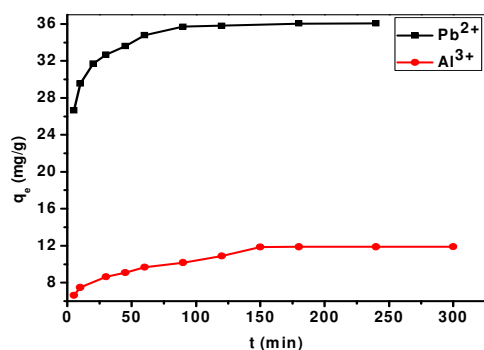


Fig. 5: Influence of contact time on removal of Pb(II) ion ( $C_1 = 50 \text{ mgg}^{-1}$ ) and Al(III) ion ( $C_1 = 20 \text{ mgg}^{-1}$ ) onto PPS

### 3.2.5. Kinetic studies

In the present study two models were used to investigate the kinetics of the the removal of Pb and Al onto PPS [29],[30].

#### Pseudo-1- order kinetic model [31]

The linearized form is given by Eq. 4:

$$\log(q_e - q_t) = \log q_e - \frac{k_1}{2.303} t \quad (4)$$

Where  $q_t$  and  $q_e$  are the amount of metal ion adsorbed per adsorbent unitmass (mgg-1) at time  $t$ (min) & at equilibrium, respectively.  $k_1$  is constant of equilibrium (1/min) that were gained from the slope & intercept of linear plots of  $\log (q_e - q_t)$  vs.  $t$  (Fig. 6a).

#### Pseudo-2- order kinetic model [31]

The linearized form can be presented by Eq. (5):

$$\frac{t}{q_e} = \frac{1}{k_2 q_e^2} + \frac{1}{q_e} t \quad (5)$$

Where,  $q_t$  and  $q_e$  are the amount of metal ion adsorbed per adsorbent unit mass (mgg<sup>-1</sup>) at time  $t$

(min) & at equilibrium, respectively.  $K_2$  is rate constant of the pseudo-second-order (g/(mg\*min)).  $q_e$  and  $k_2$  can be identified from the intercept & slope of drawing  $t/qt$  against  $t$  (Fig. 6b) [33].

**Intra-particle diffusion model** [34], [35] is expressed Eq.6 :

$$q_t = k_{int} t^{0.5} + C \quad (6)$$

Where  $k_{int}(\text{g}/\text{mg} \cdot \text{min}^{1/2})$  is the constant of adsorption, the intercept is  $C$ , both  $C$  and  $k_{int}$  are calculated by drawing  $q_t$  vs.  $t^{0.5}$  (Fig. 6c).

The Boyd kinetic data [36] is expressed by Eq.7:

$$F(t) = 1 - \frac{6}{\pi^2} \sum_{n=1}^{\infty} \frac{1}{n^2} \exp(-n^2 B t) \quad (7)$$

Where  $B(t)$  is mathematical function of  $F$ ,  $F(t)$  is the fractional achievement of equilibrium at time ( $t$ ) and is determined from Eq. 8:

$$F = \frac{q(t)}{q(e)} \quad (8)$$

Where  $q_{(e)}$  and  $q_{(t)}$  are the adsorbent capacity at equilibrium & time  $t$ , respectively.

Eq. 8 is modified to Eq. 9

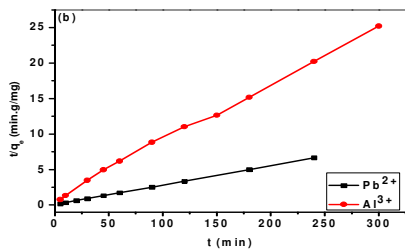
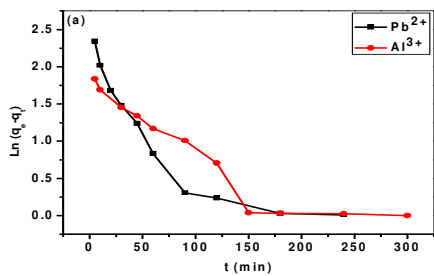
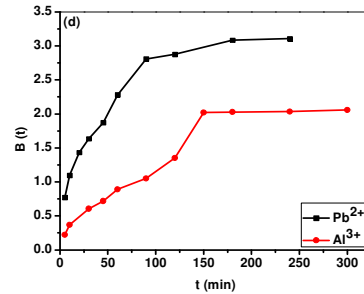
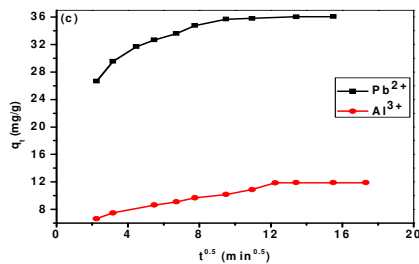
$$B(t) = \left\{ \sqrt{\pi} - \sqrt{\pi - \left\{ \frac{n^2 F(t)}{3} \right\}^2} \right\}^2 \quad (9)$$

Herein, the pseudo-1-order, pseudo-2-order, intraparticle diffusion and Boyd models were used to study the removal behavior of Pb and Al onto PPS. the results are presented in Figure 6 (a-d) and Table 2. The values of  $R^2$  revealed that the adsorption procedure is well fit with the pseudo-2- order kinetic model indicating a chemisorption mechanism of the metal ions. The intraparticle diffusion model elucidates that the removal of Pb(II) and Al(III) by PPS involved three steps; Rapid 1<sup>st</sup> step due to diffusion of Pb(II) and Al(III) to the PPS surface, linear 2<sup>nd</sup> step is the intraparticle diffusion due to , diffusion of Pb(II) and Al(III) from the PPS surface to the inside pores, and third equilibrium step. Furthermore, as it can be noticed from Figure 6c and 6d, none of the straight lines in the intraparticle diffusion and Boyd models passed through the

**Table 2**

Kinetic parameters for the adsorption of Pb(II) and Al(III) onto PPS

Model	Kinetic parameter	Metal	
		Pb(II)	Al(III)
	$q_{e, \text{exp}}$ ( $\text{mgg}^{-1}$ )	35.90	12.473
Pseudo-1-order equation	$q_{e1}$ ( $\text{mgg}^{-1}$ )	8.453	5.020
	$k_1$ ( $\text{min}^{-1}$ )	0.0182	0.0069
	$R^2_1$	0.9312	0.8605
Pseudo-2-order equation	$q_{e2}$ ( $\text{mgg}^{-1}$ )	36.50	12.392
	$K_2$ ( $\text{g/mg} \cdot \text{min}$ )	0.0099	0.00676
	$R^2_2$	0.9999	0.9972
Intra-particle diffusion equation	$K_{\text{int}}$ ( $\text{mgg}^{-1} \cdot \text{min}^{1/2}$ )	0.6307	0.3672
	$C$	28.273	6.5221
	$R^2_{\text{int}}$	0.7606	0.9221
Boyd equation	Intercept	1.3266	0.446
	$R^2$	0.7802	0.8605

**Fig. 6:** Kinetic models for adsorption of lead(II) and aluminium(III) by PPS (a) pseudo-1-order, (b) pseudo-2-order,**Fig. 6:** Kinetic models for adsorption of lead(II) and aluminium(III) by PPS (c) intraparticle diffusion and (d) Boyd model

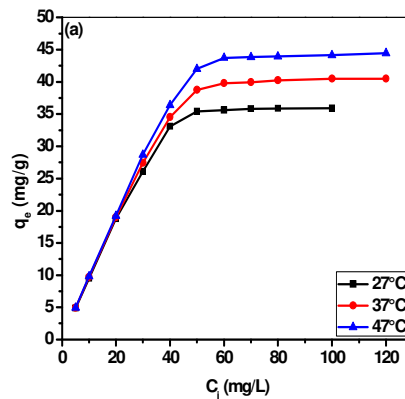
### 3.2.6. Influence of temperature

The influence of temperature on removal% was studied at 27, 37 and 47°C. The results are presented in Figure 7 and Table 3. As it can be noticed, the maximum amounts of Pb(II) & Al(III) removed by PPS are found to increase from 35.9  $\text{mgg}^{-1}$  to 44.47  $\text{mgg}^{-1}$  and from 12.47  $\text{mgg}^{-1}$  to 15.38  $\text{mgg}^{-1}$  as the temperature rises from 27 to 47 °C, respectively. The increase in adsorption capacity may be brought about by chemical reactions between PPS sites and metal ions or by the raised rate of Pb(II) and Al(III) molecule intraparticle diffusion into the carbon pores at higher temperatures[37].

**Table 3**

Influence of temperature on adsorption capacities of Pb(II) and Al(III) by PPS

Metal	$Q_{\text{max}}$ ( $\text{mgg}^{-1}$ )		
	27°C	37 °C	47 °C
Pb(II)	35.900	40.510	44.470
Al(III)	12.473	14.083	15.378



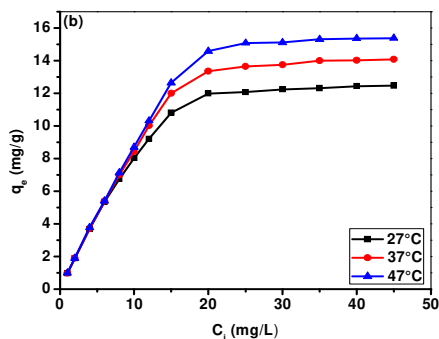


Fig. 7: Influence of temperature on maximum capacities of (a)  $Pb^{2+}$  and (b)  $Al^{3+}$  ions by PPS

### 3.2.7. Thermodynamic studies of Pb(II) and Al(III) by PPS

The thermodynamic parameters including Gibbs free energy ( $\Delta G^0$ ), enthalpy ( $\Delta H^0$ ), and entropy ( $\Delta S^0$ ) are determined by Eq. 11 & 12

$$\Delta G^0 = -RT \ln k_d \quad (11)$$

$$\ln k_d = \frac{-\Delta H^0}{RT} + \frac{\Delta S}{R} \quad (12)$$

Where,  $K_d$  is Langmuir constant, R is gas constant (8.314 J/mol K) and T is the temperature (K), respectively.

The ( $\Delta S^0$ ) and ( $\Delta H^0$ ) values are gained from the intercept & slope of  $\ln K_d$  versus  $1/T$  plot (Van't Hoff), Figure 8. The plot of  $\ln K_d$  versus  $1/T$  (Figure 8) was linear over the temperature range used. The thermodynamic parameters are presented in Table 4. Analysis of the data in Table 4 revealed that the adsorption of Pb and Al onto PPS is an endothermic (+ve  $\Delta H^0$ ) and spontaneous process (-ve  $\Delta G^0$ )[38].

Table 4: Thermodynamics Parameters for the adsorption of Pb(II) and Al(III) on PPS

Metal	$\Delta H^0$ (KJ/mol)	$\Delta S^0$ (KJ/mol)	$\Delta G^0$ (KJ/mol)		
			27°C	37°C	47°C
Pb(II)	30.4043	0.1087	-2.2115	-3.1846	-4.4156
Al(III)	23.3939	0.0813	-1.0056	-1.7979	-2.6327

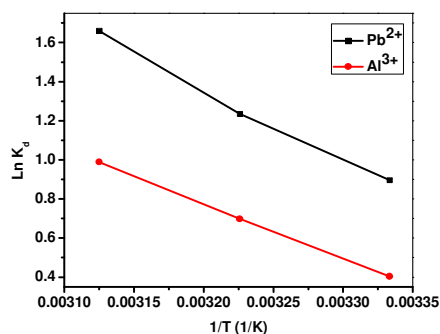


Fig. 8: Van't Hoff isotherm for removal of Pb(II) and Al(III) onto PPS

### 3.2.8. Adsorption Isotherms

#### Langmuir isotherm model

The linear form of Langmuir isotherm model is given by Eq.13 [36]:

$$\frac{C_e}{q_e} = \frac{1}{k_L q_m} + \frac{C_e}{q_m} \quad (13)$$

Where,  $q_e$  is the adsorption capacity of metal ion at equilibrium ( $mgg^{-1}$ ),  $q_m$  is the theoretical maximum capacity of adsorption ( $mgg^{-1}$ ),  $C_e$  is the amount of metal at equilibrium ( $mg/L$ ) and  $k_L$  is Langmuir constant ( $L/mg$ ).

The Langmuir isotherm plot is obtained by plotting  $C_e/q_e$  against  $C_e$  (Figure 9a)...

The fundamental characteristics of the Langmuir isotherm can be expressed by a dimensionless separation factor,  $R_L$ , given in Eq.14

$$R_L = \frac{1}{1 + K_L C_0} \quad (14)$$

Where  $K_L$  is Langmuir constant and  $C_0$  is the highest initial metal concentration ( $mgL^{-1}$ ). The  $R_L$  value can give an idea about the type of the isotherm: ( $R_L > 1$ ), unfavourable; ( $R_L = 1$ ), linear; ( $0 < R_L < 1$ ), favourable; ( $R_L = 0$ ), irreversible. (Table 5). In our study, the values of ( $R_L$ ) in the present study are less than 1 confirming that PPS adsorbent exhibits favorable metal ion adsorption

#### Freundlich model [39]

The adsorption isotherms of adsorption of Pb(II) and Al(III) onto PPS is shown in Figure 9b [39].

The linear form of Freundlich Isotherm can be presented as in Eq. 15:

$$\log q_e = \log K_F + \frac{1}{n} \log C_e \quad (15)$$

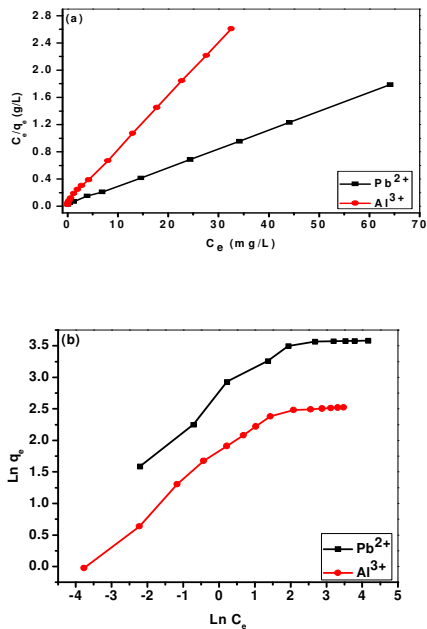
Where  $K_F$  and  $n$  are Freundlich constants,  $K_F$  and  $n$  are the indicator of adsorption capacity and adsorption intensity, respectively (Fig. 9b).

Table 5  
Langmuir and Freundlich isotherm Parameters

M	Langmuir parameters				Freundlich parameters		
	$q_m$ (mg/g)	$K_L$ (L/mg)	$R_L$	$R^2$	$n$	$K_F$	$R^2$
Pb	36.630	1.0074	0.0109	0.9997	3.242	13.294	<b>0.8841</b>
Al	12.771	1.2448	0.0158	0.9989	2.906	5.0506	<b>0.9202</b>

The calculated results of isotherm parameters are shown in Table 5. According to the values of  $R^2$ , it is strongly suggested that the adsorption of Pb(II) and Al(III) onto PPS fits well with the Langmuir isotherm

and the adsorption is a monolayer adsorption and takes place on homogeneous surfaces.



**Fig. 9 :** (a) Langmuir and (b) Freundlich plot for the adsorption  $Pb^{2+}$  and  $Al^{3+}$  by PPS

### 3.2.9. The influence of foreign ions

The influence of different foreign cations such as calcium  $Ca^{2+}$ ,  $Mg^{2+}$ ,  $Na^+$ ,  $K^+$  and  $Na^+$  as well as anions ( $F^-$ ,  $Cl^-$ , acetate and oxalate) on the adsorption of  $Pb(II)$  and  $Al(III)$  using PPS was estimated. The results in Table 6, show that the studied anions and cations do not interfere in the removal % of  $Pb(II)$  and  $Al(III)$  on the PPS, up to  $200\text{ mgL}^{-1}$ .

**Table 6**

Influence of interferents on the removal percentage of  $Pb(II)$  and  $Al(III)$  onto PPS

Foreign ion (200 mg/L)	R%	
	Pb(II)	Al(III)
$F^-$	96.86	94.33
$Cl^-$	98.43	93.80
Acetate	98.77	91.857
Oxalate	84.31	87.89
$Mg^{2+}$	71.95	66.6
$Ca^{2+}$	74.95	69.80
$Na^+$	99.77	93.73
$K^+$	95.29	93.86

### 3.2.10. Influence of NaCl

The influence of NaCl on the adsorption of  $Pb(II)$  and  $Al(III)$  is presented in Figure 10. It was shown that when ionic strength increased, the adsorption capacity decreased. The adsorption capabilities fell from  $32.74$  to  $28.32\text{ mgg}^{-1}$ , from  $9.209$  to  $9.007\text{ mgg}^{-1}$  for  $Pb^{2+}$  and  $Al^{3+}$ , respectively, when the concentration of NaCl increased from  $0.01$  to  $0.2\text{ M}$ .  $Pb^{2+}$  and  $Al^{3+}$  and  $Na^+$  cations may have been competing with one another for the active sites on the adsorbent surface, which could account for this.

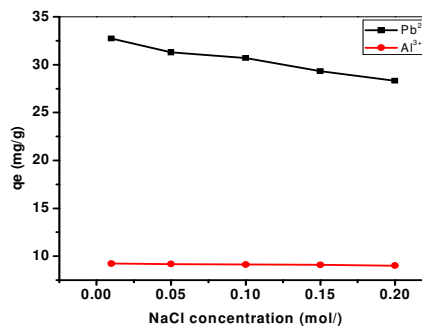


**Fig. 10:** Influence of NaCl on the adsorption of  $Pb(II)$  ( $C_e=50\text{ mgL}^{-1}$ ) and  $Al(III)$  ions ( $C_e=12\text{ mgL}^{-1}$ ) by PPS

### 3.2.11. Desorption studies

Desorption of  $Pb(II)$  and  $Al(III)$  from the metal ion loaded PPS was performed using  $0.05$ ,  $0.10$  and  $0.20\text{ M}$  HCl. The percentage of desorption with  $0.20\text{ M}$  of HCl is shown to be  $97.19$  and  $96.60\%$  for  $Pb(II)$  and  $Al(III)$ , respectively, Table 7.

## 4. Conclusion

The present study investigates the adsorption of  $Pb(II)$  and  $Al(III)$  on PPS. The following results have been obtained:

- (1) Precursor Pistachio Shells(PPS) can be a suitable adsorbent for the removal of  $Pb(II)$  and  $Al(III)$  from real water samples
- (2) The adsorption of  $Pb(II)$  and  $Al(III)$  on PPS was found to be pH-dependent
- (3) The adsorption increased with the increase in dosage of the adsorbent.
- (4) The pseudo-2- order kinetic model agrees very well with the dynamic behavior for the adsorption of  $Pb(II)$  and  $Al(III)$  from aqueous solution onto PPS.
- (6) Thermodynamic parameters suggested that the adsorption of  $Pb(II)$  and  $Al(III)$  on PPS is of a spontaneous and endothermic nature.

**Table 7**

Desorption % of Pb(II) and Al(III) ions from PPS adsorbent

Adsorbate (Metal)	q <sub>e</sub> Adsorbed (mgg <sup>-1</sup> )	HCl (molL <sup>-1</sup> )					
		0.05		0.1		0.2	
		q <sub>e</sub> desorbed (mgg <sup>-1</sup> )	D %	q <sub>e</sub> desorbed (mgg <sup>-1</sup> )	D%	q <sub>e</sub> desorbed (mgg <sup>-1</sup> )	D %
Pb(II)	33.10	21.29	64.32	31.75	95.93	32.17	97.19
Al(III)	6.76	4.31	63.76	6.44	95.22	6.53	96.6

## 5. References

- [1] C. G. Friberg, L., Elinder, *Encyclopedia of Occupational Health, International Labor Organization*, Third ed. Geneva, 1985.
- [2] D. Sud, G. Mahajan, and M. P. Kaur, "Agricultural waste material as potential adsorbent for sequestering heavy metal ions from aqueous solutions – A review," vol. 99, pp. 6017–6027, 2008.
- [3] E. Yoshimura, M. Kashi, and K.-I. Tsunoda, *Anal. Sci.*, **2004**, 20, 373.
- [4] W. L. Lindsay and Walthal, "The Environmental Chemistry of Aluminum", ed. G. Sposito, 2nd ed., **1996**, CRC Press, Boca Raton, Florida, 334.
- [5] C. T. Driscoll Jr. and K. M. Postek, "The Environmental Chemistry of Aluminum", ed. G. Sposito, 2nd ed., **1996**, CRC Press, Boca Raton, Florida, 363.
- [6] F. N. Kemmer, "Nalco Water Handbook", 2nd ed., **1988**, Mc-Graw-Hill, New York.
- [7] C. T. Driscoll Jr. and K. M. Postek, "The Environmental Chemistry of Aluminum", ed. G. Sposito, 2nd ed., **1996**, CRC Press, Boca Raton, Florida, 363.
- [8] R. L. Bensen, P. J. Worsfold, and F. W. Sweeting, *Anal. Chem. Acta*, **1990**, 238, 17.
- [9] P. G. C. Campbell, M. Bisson, R. Bougie, A. Tessier, and J.-P. Villeneuve, *Anal. Chem.*, **1983**, 55, 2246.
- [10] J. D. Birchall, C. Exley, J. S. Chappell, and M. J. Phillips, *Nature* [London], **1989**, 338, 46.
- [11] K. E. Havens and R. T. Heath, *Environ. Pollut.*, **1989**, 62, 195.
- [12] K. E. Havens, *Can. J. Aquat. Fish Sci.*, **1992**, 49, 2392.
- [13] S. H. Lin, R. S. Juang, Heavy Metal Removal from Water by Sorption Using Surfactant-Modified Montmorillonite, *J. Hazard. Mater.* 2002, B92, 315–326.
- [14] M. N. M. Ibrahim, W. S. W. Ngah, M. S. Norliyana, W. R. W. Daud, Copper(II) Biosorption on Soda Lignin from Oil Palm Empty Fruit Bunches (EFB), *Clean: Soil Air Water* 2009, 37 (1), 80–85.
- [15] O. Demirbas, A. Karadag, M. Alkan, M. Dogan, Removal of Copper Ions from Aqueous Solutions by Hazelnut Shell, *J. Hazard. Mater.* 2008, 153, 677–684.
- [16] O. Gok, A. S. Ozcan, A. Ozcan, Adsorption Kinetics of Naphthalene onto Organo-Sepiolite from Aqueous Solutions, *Desalination* 2008, 220, 96–107.
- [17] M. S. O'lenner, S. Tunali, A. S. Ozcan, A. Ozcan, T. Gedikbey, Adsorption Characteristics of Lead(II) Ions onto the Clay/Poly(methoxyethyl) Acrylamide (PMEA) Composite from Aqueous Solutions, *Desalination* 2008, 223, 308–322.
- [18] T. Tay, M. Candan, M. Erdem, Y. Cimen, H. Turk, Biosorption of Cadmium Ions from Aqueous Solution onto Non-Living Lichen *Ramalina fraxinea* Biomass, *Clean: Soil Air Water* 2009, 37 (3), 249–255.
- [19] S. E. Bailey, J. T. Olin, R. M. Bricka, D. D. Adrian, A Review of Potentially Low-Cost Sorbents for Heavy Metals, *Water Res.* 1999, 33 (1), 2469–2479.
- [20] K. S. Low, C. K. Lee, A. C. Leo, Removal of Metals from Electroplating Wastes Using Banana Pith, *Bioresour. Technol.* 1995, 51, 227–231.
- [21] S. P. Mishra, D. Tiwari, R. S. Dubey, The Uptake Behavior of Rice (Jaya) Husk in the Removal of Zn(II) Ions: A Radiotracer Study, *Appl. Radiat. Isot.* 1997, 48, 877–882.
- [22] F. R. Zaggout, Removal of Copper from Water by Decaying *Tamrix gallica* Leaves, *Asian J. Chem.* 2001, 13, 639–650
- [23] L. R. Radovic, P. L. Walker, and R. G. Jenkins, "Importance of carbon active sites in the gasification of coal chars," *Fuel*, vol. 62, no. 7, pp. 849–856, 1983.
- [24] C. A. Leon y Leon, J. M. Solar, V. Calemma, and L. R. Radovic, "Evidence for the protonation of basal plane sites on carbon," *Carbon N. Y.*, vol. 30, no. 5, pp. 797–811, 1992.
- [25] Y. F. Jia, B. Xiao, and K. M. Thomas,

- “Adsorption of metal ions on nitrogen surface functional groups in activated carbons,” *Langmuir*, vol. 18, no. 2, pp. 470–478, 2002.
- [25] F. Stoeckli and D. Hugi-Cleary, “On the mechanisms of phenol adsorption by carbons,” *Russ. Chem. Bull.*, vol. 50, no. 11, pp. 2060–2063, 2001.
- [26] P. Vijayalakshmi, V. S. S. Bala, K. V. Thiruvengadaravi, P. Panneerselvam, M. Palanichamy, and S. Sivanesan, “Removal of Acid Violet 17 from Aqueous Solutions by Adsorption onto Activated Carbon Prepared from Pistachio Nut Shell,” *Sep. Sci. Technol.*, vol. 46, no. 1, pp. 155–163, 2010.
- [27] M. A. I. Ayman Atta, Abd ElFattah M Youssef, “The Utility of Novel Superabsorbent Core Shell Magnetic Nanocomposites for Efficient Removal of Basic Pb and Als from Aqueous Solutions,” *J. Chromatogr. Sep. Tech.*, vol. 4, no. 5, pp. 2–9, 2013.
- [28] E. O. Oyelude and F. Appiah-Takyi, “Removal of methylene blue from aqueous solution using alkali-modified malted sorghum mash,” *Turkish J. Eng. Environ. Sci.*, vol. 36, no. 2, pp. 161–169, 2012.
- [29] J.-J. Gao, Y.-B. Qin, T. Zhou, D.-D. Cao, P. Xu, D. Hochstetter, and Y.-F. Wang, “Adsorption of methylene blue onto activated carbon produced from tea (*Camellia sinensis* L.) seed shells: kinetics, equilibrium, and thermodynamics studies,” *J. Zhejiang Univ. Sci. B*, vol. 14, no. 7, pp. 650–8, 2013.
- [30] A. Demirbas, “Oil from Tea Seed by Supercritical Fluid Extraction,” *Energy Sources, Part A Recover. Util. Environ. Eff.*, vol. 31, no. 3, pp. 217–222, 2009.
- [31] B. H. Hameed, A. L. Ahmad, and K. N. A. Latiff, “Adsorption of basic Pb and Al (methylene blue) onto activated carbon prepared from rattan sawdust,” *J. Hazard. Mater.*, vol. 75, no. 1, pp. 143–149, 2006.
- [32] A. S. Franca, L. S. Oliveira, and M. E. Ferreira, “Kinetics and equilibrium studies of methylene blue adsorption by spent coffee grounds,” *Desalination*, vol. 249, no. 1, pp. 267–272, 2009.
- [33] G. Annadurai, R. S. Juang, and D. J. Lee, “Use of cellulose-based wastes for adsorption of Pb and Als from aqueous solutions,” *J. Hazard. Mater.*, vol. 92, no. 3, pp. 263–274, 2002.
- [34] F. C. Wu, R. L. Tseng, and R. S. Juang, “Adsorption of Pb and Als and phenols from water on the activated carbons prepared from corncob wastes,” *Environ. Technol.*, vol. 22, no. 2, pp. 205–13, 2001.
- [35] G. E. Boyd, a W. Adamson, and L. S. Myers, “The exchange adsorption of ions from aqueous solutions by organic zeolites; kinetics,” *J. Am. Chem. Soc.*, vol. 69, no. 11, pp. 2836–2848, 1947.
- [36] Y. Kismir and A. Z. Aroguz, “Adsorption characteristics of the hazardous Pb and Al Brilliant Green on Sakli{dotless}kent mud,” *Chem. Eng. J.*, vol. 172, no. 1, pp. 199–206, 2011.
- [37] M. A. A. Akl, M. B. Dawy, and A. A. Serage, “Efficient Removal of Phenol from Water Samples Using Sugarcane Bagasse Based Activated Carbon,” *J Anal Bioanal Tech*, vol. 5, no. 2, pp. 2–12, 2014.
- [38] I. Langmuir, “THE ADSORPTION OF GASES ON PLANE SURFACES OF GLASS, MICA AND PLATINUM,” *J. Am. Chem. Soc.*, vol. 40, no. 9, pp. 1361–1403, Sep. 1918.
- [39] H. M. F. Freundlich, “Over the Adsorption in Solution,” *Zeitschrift fur Phys. Chemie*, vol. 57, pp. 385–470, 1906.